Direct Physical Measure of Conformational Rearrangement Underlying Potassium Channel Gating

Lidia M. Mannuzzu, Mario M. Moronne, Ehud Y. Isacoff*

In response to membrane depolarization, voltage-gated ion channels undergo a structural rearrangement that moves charges or dipoles in the membrane electric field and opens the channel-conducting pathway. By combination of site-specific fluorescent labeling of the *Shaker* potassium channel protein with voltage clamping, this gating conformational change was measured in real time. During channel activation, a stretch of at least seven amino acids of the putative transmembrane segment S4 moved from a buried position into the extracellular environment. This movement correlated with the displacement of the gating charge, providing physical evidence in support of the hypothesis that S4 is the voltage sensor of voltage-gated ion channels.

Since voltage-gated ion channels were first cloned, it has been postulated that the positively charged S4 segment functions as the voltage sensor (*1*). Membrane depolarization is hypothesized to open the channel by moving S4 outward, thus generating the gating current. In keeping with this model, mutations that alter the charge of amino acids in S4 were shown in several studies to affect the voltage sensitivity of channel opening (*2*, *3*). However, these studies could not prove that S4 contains the gating charge because the voltage sensitivity of channel opening can also be affected by changes in the cooperativity or equilibria of gating transitions (*4*). In the S4 region of a skeletal muscle Na^+ channel, one amino acid position has increased accessibility to the extracellular solution during membrane depolarization (*5*). This suggests that S4 may move, without explaining how or during which gating transition (activation, opening, or inactivation). The primary prediction of the S4 hypothesis—a correlation between S4 movement and movement of the gating charge—remains to be tested.

To address this problem, we developed a fluorescence technique to study conformational changes of the *Shaker* K^+ channel S4 during gating in *Xenopus* oocytes. This technique relies on the sensitivity of many fluorophores to their local environment and on the short lifetime of their excited state (*6*). Fluorescent labels conjugated to residues in S4 could report changes in the environment if activation moves them from a position buried in the membrane into the extracellular fluid, as has been proposed (*4*, *7*). To covalently label the channel with a fluorophore (*8*), we substituted cysteine at positions 346, 356, 359, 365, and 366 (Fig. 1A) of a nonconducting (W434F) (*9*), noninactivating (Δ6–46) (*10*) version of the *Shaker* ShH4 K^+ channel (*11*), after removing two native cysteines (C245V in S1 and C462A in S6), which could be accessible to the external solution (*12*). Cysteines present in endogenous oocyte plasma membrane proteins were blocked with a nonfluorescent and impermeant maleimide (*8*). Oocytes injected with comparable amounts of complementary RNA encoding each of the mutant channels were labeled with the membrane-impermeant dye tetramethylrhodamine-maleimide (TMRM) (*8*), and membrane fluorescence was quantitated by confocal microscopy (Fig. 1B). Integration of the fluorescence over the focused membrane area showed between 2.5- and 5.0-fold greater labeling ($P < 0.0001$) of the plasma membrane of oocytes expressing the cysteine-added mutants compared with both uninjected oocytes and oocytes expressing the cysteine-removed control channel (Fig. 1C). The degree of labeling was comparable for S346C, M356C, A359C, and R365C, but it was significantly lower ($P < 0.02$) for the position furthest toward the COOH-terminal end of S4 (L366C) (Fig. 1, B and C). Because

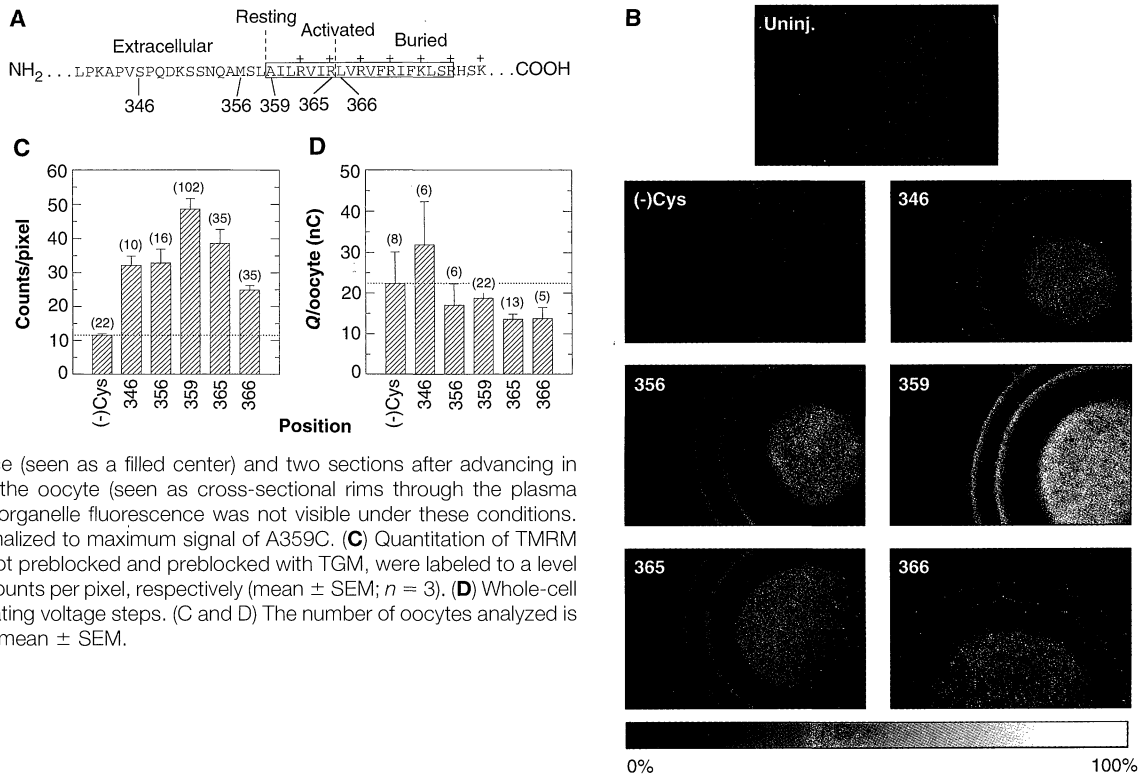

Fig. 1. Fluorescent labeling of *Shaker* cysteine-added mutants. (**A**) *Shaker* S4 sequence, with sites of cysteine substitution, and standard prediction of membrane-spanning segment (box) (*7*, *12*). Dashed lines indicate minimal movement required to explain the change in S4 exposure during activation. (**B**) Confocal images of TMRM-labeled uninjected oocytes (Uninj.) and oocytes expressing cysteine-removed control [(−)Cys] or cysteine-added mutant channels. Three optical sections are superimposed: the oocyte surface (seen as a filled center) and two sections after advancing in successive 30-μm steps into the oocyte (seen as cross-sectional rims through the plasma membrane). Cytoplasmic and organelle fluorescence was not visible under these conditions. Scaling of color map was normalized to maximum signal of A359C. (**C**) Quantitation of TMRM labeling. Uninjected oocytes, not preblocked and preblocked with TGM, were labeled to a level of 90.2 ± 5.1 and 14.4 ± 1.5 counts per pixel, respectively (mean ± SEM; $n = 3$). (**D**) Whole-cell gating charge evoked by saturating voltage steps. (C and D) The number of oocytes analyzed is in parentheses. Values are the mean ± SEM.

the channel density of L366C, as judged by measurement of whole-cell gating currents (Fig. 1D) (8), was similar to that of the other cysteine-added mutants, the lower level of L366C labeling is probably due to a lower accessibility of this position to external TMRM. Specific labeling of the cysteine-added mutants was confirmed by fluorescence analysis of membrane proteins from labeled oocytes, immune-precipitated and separated by polyacrylamide gel electrophoresis, which showed a broad rhodamine-labeled band of 110 to 115 kD (corresponding to the completely glycosylated *Shaker* protein) (*13*) present only in these mutants (*14*).

The model proposed for K^+ channel gating suggests that a portion of S4 that is buried in the resting state becomes exposed to the external solution by activation (*7*). To test this model, we incubated oocytes expressing S346C, A359C, and R365C with TMRM in a hyperpolarizing NMGMES solution [resting membrane potential (V_{rest}) = −58.7 ± 11.6 mV; mean ± SD; n = 12] and a depolarizing K^+-MBSH solution (V_{rest} = −1.2 ± 5.4 mV; mean ± SD; n = 17) (*8*). The charge-voltage (*Q-V*) relations measured for these mutants indicated that S346C and A359C would be primarily in the resting state in NMGMES but would be activated most of the time in K^+-MBSH, whereas R365C would also be in the resting state in NMGMES but only be activated about 40% of the time in K^+-MBSH (Fig. 2A). Under these conditions, S346C was equally labeled when depolarized or hyperpolarized, A359C was significantly more labeled ($P < 0.005$) when depolarized, and R365C was labeled when depolarized but not when hyperpolarized (Fig. 2B). Thus, membrane depolarization increased the exposure of positions 359 and 365 to the extracellular solution, whereas position 346 was equally exposed under depolarizing and hyperpolarizing conditions (*15*). The partial labeling of A359C in the hyperpolarizing solution may be due to the fact that it was activated about 10% of the time in this solution (Fig. 2A).

During the prolonged depolarization of the K^+-MBSH incubation, channels are expected to spend part of their time in the C-type inactivated state (*16*). To determine whether it is activation, rather than C-type inactivation, that increases the surface exposure of S4, we examined the effect of short depolarizations (producing no C-type inactivation) on S4 access to the extracellular solution. We monitored surface exposure of S4 by exploiting the sensitivity of fluorophores to the polarity of their environment (*6*). For TMRM, increasing the polarity of the solvent from ethanol (dielectric constant ε = 24) to water (ε = 78) decreased peak fluorescence by 33% and shifted the peak from 567 to 575 nm. This indicated that it should be possible to observe a change in

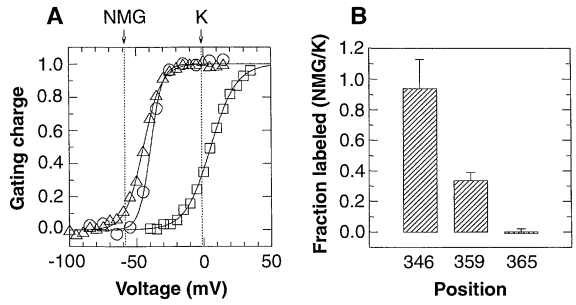

Fig. 2. State dependence of S4 labeling. (**A**) Normalized *Q-V* relation for S346C (circles), A359C (triangles), and R365C (squares). Gating charge was recorded in NMGMES. Dashed lines indicate average membrane potential measured upon impalement in NMGMES (NMG) or in K^+-MBSH (K). (**B**) Ratio of labeling in NMGMES over labeling in K^+-MBSH. Labeling was as described in (*8*) (7 to 10 oocytes were used for each mutant in each labeling condition). Values are the mean ± SEM.

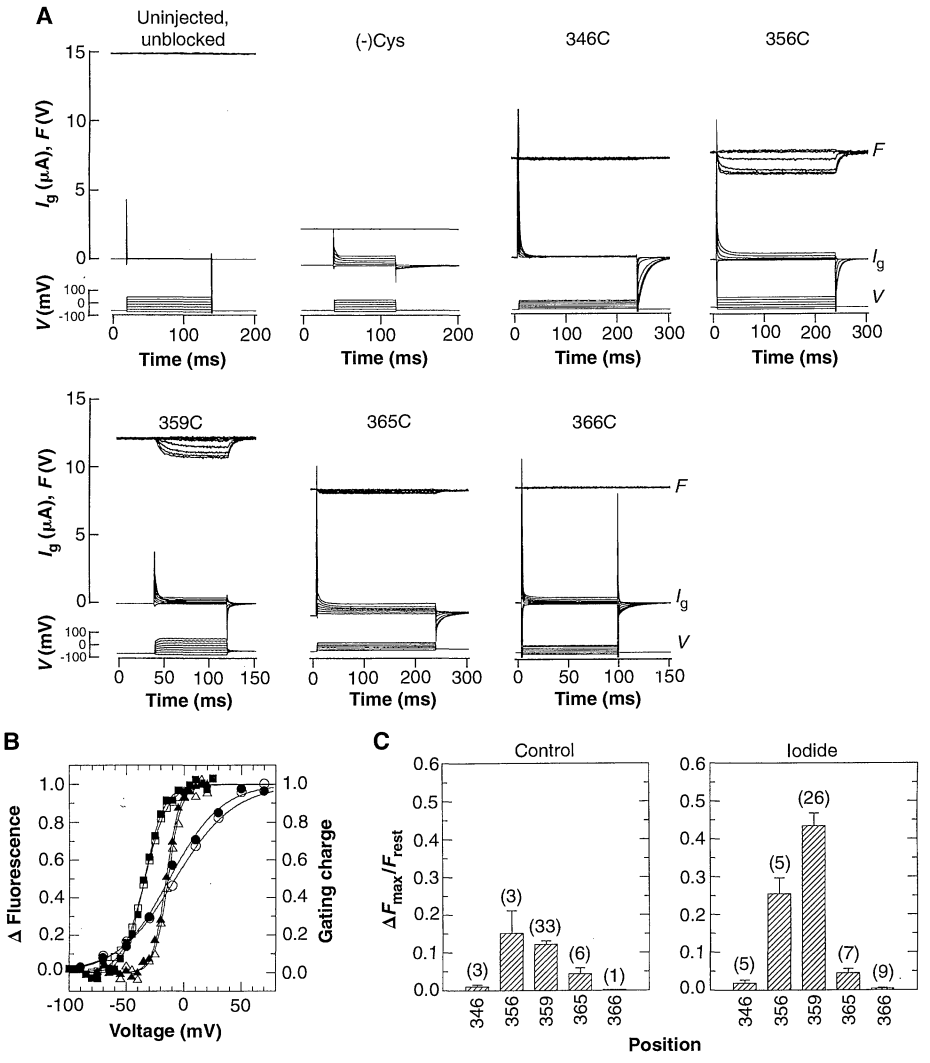

Fig. 3. Voltage-dependent fluorescence change of TMRM-labeled S4 mutants. (**A**) Simultaneous fluorescence (*F*, top traces) and gating current (I_g, middle traces) measurements during voltage steps (*V*, bottom traces). Background fluorescence of cysteine-removed control was subtracted from fluorescence records. Current records were not leak subtracted. Uninjected oocytes were not first blocked with TGM, yielding TMRM labeling of native oocyte cysteines. (**B**) Correspondence between the normalized *F-V* (filled symbols) and *Q-V* (open symbols) for single oocytes expressing M356C (triangles), A359C (squares), and R365C (circles), fit to single Boltzmann equations (solid lines). (**C**) Maximal fluorescence change (ΔF_{max}) at a saturating voltage step, as a fraction of fluorescence at holding potential minus fluorescence of cysteine-removed control (F_{rest}), either in Na^+-MBSH (control) or in K^+-MBSH with 50 mM KCl replaced by 50 mM KI (iodide). The number of oocytes is in parentheses. Values are the mean ± SEM.

L. M. Mannuzzu and E. Y. Isacoff, Department of Molecular and Cell Biology, 229 Stanley Hall, University of California, Berkeley, CA 94720, USA.
M. M. Moronne, Lawrence Berkeley Laboratory, Berkeley, CA 94720, USA.
*To whom correspondence should be addressed.

fluorescence if TMRM, conjugated to S4, moved into the polar extracellular fluid from a buried, less polar environment.

To examine the relation between changes in the environment of S4 and gating charge displacement, we measured fluorescence of labeled oocytes and whole-cell gating current in parallel under two-electrode voltage clamp (*17*). At negative holding potentials, membrane fluorescence was higher for oocytes expressing the cysteine-added mutants compared with cysteine-removed controls (Fig. 3A) and uninjected oocytes (*14*). On average, the fluorescence at a negative holding potential of −80 mV was comparable for the S346C, M356C, A359C, and R365C mutants but lower for the L366C mutant, which is in agreement with the confocal measurements (Fig. 1). A series of depolarizing voltage steps moved gating charge for each of the mutants. For several of the mutants, the steps evoked a graded and saturating decrease in fluorescence, which followed the kinetics of the gating current (Fig. 3A). The maximal decrease in fluorescence was about 10% for M356C and A359C and 5% for R365C. There was almost no change for S346C (<1%), and no fluorescence change was observed for L366C, or for uninjected oocytes whose endogenous membrane sulfhydryls were left unblocked before labeling with TMRM (Fig. 3, A and C). For the mutants with the largest fluorescence change (M356C, A359C, and R365C), the fluorescence-voltage relation (*F-V*) was closely correlated with the *Q-V* (Fig. 3B) but not with the voltage dependence of channel opening measured from these mutants in a conducting background (*14*). It is unlikely that the observed fluorescence changes were due to a direct effect of the voltage-clamp steps on the energy levels of TMRM, because field perturbations of the fluorophore would be expected neither to saturate nor to correlate with gating charge movement. Instead, these fluorescence decreases most likely reflect a change in the environment of the fluorophore tethered to residues 356, 359, or 365 when these sites move during activation. These results indicate that channel activation, rather than inactivation or opening, is responsible for the observed increase in S4 exposure to extracellular TMRM (Fig. 2).

If the fluorescence decrease is caused by the movement of TMRM conjugated at sites 356 to 365 from a position buried within the membrane into the extracellular solution, then extracellular quenchers should enhance the fluorescence decrease. To test this hypothesis, we examined the effect of external iodide, a membrane-impermeant collisional quencher (*18*). Iodide enhanced the fluorescence change of A359C by 3.6-fold ($P < 10^{-5}$) but did not significantly affect the fluorescence change of the other mutants (Fig. 3C), although the small sample size may explain the lack of significance observed with M356C. Thus, activation clearly exposes TMRM conjugated at A359C to extracellular iodide.

Several biophysical models have been constructed to explain the gating of the *Shaker* K^+ channel (*4, 19–21*). These models, based on ionic and gating-current measurements, propose two or more major sets of charge-carrying transitions. To investigate further the relation between movement of S4 and movement of the gating charge, we examined the effect on the 359C fluorescence of the S4 mutation L382V, which alters just one of the charge-carrying steps in channel activation (*3, 4, 20*). The double mutant A359C/L382V had an effect similar to that described earlier for L382V alone (*3, 4, 20*); it accelerated gating current kinetics (Fig. 4B) and decreased the slope of the *Q-V* (Fig. 4E). Unlike L382V, however, the *Q-V* of A359C/L382V was not resolved into two clearly separated components, possibly as a result of the A359C mutation or the TMRM conjugation. As with the gating current, A359C/L382V accelerated the rate of the fluorescence change (Fig. 4, A to D), and the slope of the *F-V* was decreased in parallel to that of the *Q-V* (Fig. 4, E and F). This observation indicates that the change in the environment of S4 follows all of the movement of the gating charge, even in a mutant that shifts one component of the charge movement.

In summary, we find that (i) L366C is less efficiently conjugated by TMRM than the other sites that we have examined; (ii) conjugation by TMRM of A359C and R365C, but not of S346C, is increased by depolarization; (iii) M356C, A359C, and R365C show a fluorescence change that correlates with gating charge displacement, whereas S346C and L366C show little or no fluorescence change; and (iv) TMRM conjugated at A359C becomes accessible to iodide upon activation. These observations are consistent with the model that S4 contains the gating charge and that activation consists of the movement of the outer (NH_2-terminal) portion of S4 into the extracellular fluid from a position that is buried in the resting state, thus generating the gating current (Fig. 1A). In this process, a stretch of at least 10 residues (356 to 365), about half of the 19 residues commonly predicted to make up S4 (*7*), experiences a change in environment. For at least seven of these residues (359 to 365) the change in exposure to the extracellular fluid is sufficiently extreme to govern whether the site can be conjugated by TMRM. A residue on the NH_2-terminal side of this stretch (346) is always exposed, whereas one on the COOH-terminal side (366) remains partly buried even when the channel is activated. This large-scale S4 movement agrees in essence with the model proposed by Durell and Guy (*7*) and is consistent with the large charge movement that occurs during gating (12 to 16 charges per channel) (*3, 4, 21, 22*).

To date, the only structural information available about the nature of the conformational change associated with ion channel gating has been for the bactericidal protein colicin Ia (*23*), nicotinic acetylcholine receptor (*24*), and the Na^+ channel (*5*). These

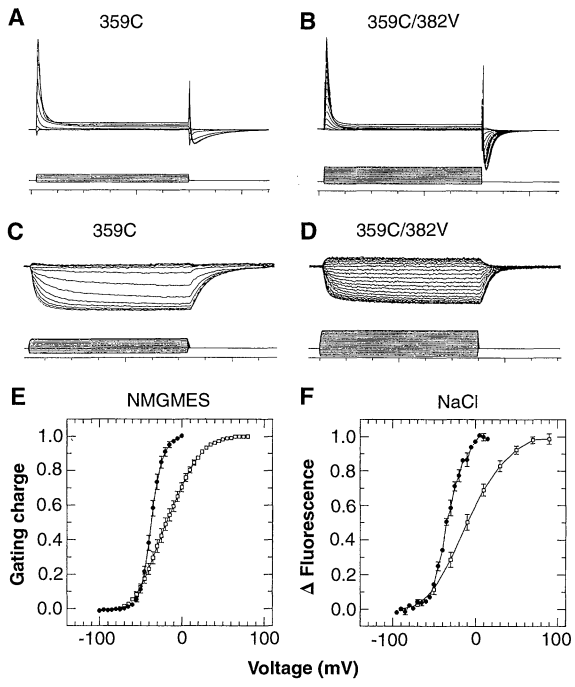

Fig. 4. Mutation L382V produces parallel changes in *Q-V* and *F-V* relations. (**A** and **B**) Normalized gating currents of A359C and A359C/L382V. Holding potential, −80 mV; tail potential, −60 mV in NMGMES. (**C** and **D**) Normalized fluorescence changes for A359C and A359C/L382V. Holding and tail potentials are −60 and −80 mV in MBSH-KI. (A through D) Voltage steps are in 10-mV increments. Each tick on the *x* axis is 20 ms. (**E**) Normalized *Q-V* relations for A359C (filled circles, n = 10) and A359C/L382V (open squares, n = 6) in NMGMES. (**F**) Normalized *F-V* relations for A359C (filled circles, n = 2) and for A359C/L382V (open squares, n = 6) in Na^+-MBSH. Values are the mean ± SEM.

studies were limited to a comparison of the end points of the gating conformations. The fluorescence technique described here provides information about the transition through conformational intermediates between these end points by tracking, with submillisecond resolution, the motion of specific domains of the channel protein as gating proceeds. This technique, in conjunction with labeling at other locations, should aid in the structural characterization of gating domains and shed light on conformational rearrangements that have so far been "invisible" because they neither move charge nor directly open or close the channel.

REFERENCES AND NOTES

1. M. Noda *et al.*, *Nature* **312**, 121 (1984); W. A. Catterall, *Annu. Rev. Biochem.* **55**, 953 (1986); R. E. Greenblatt, T. Blatt, M. Montal, *FEBS Lett.* **193**, 125 (1985); H. R. Guy and P. Seetharamulu, *Proc. Natl. Acad. Sci. U.S.A.* **83**, 508 (1986).
2. W. Stühmer *et al.*, *Nature* **339**, 597 (1989); D. M. Papazian, L. C. Timpe, Y. N. Jan, L. Y. Jan, *ibid.* **349**, 305 (1991); E. R. Liman, P. Hesse, F. W. Weaver, G. Koren, *ibid.* **353**, 752 (1991); D. E. Logothetis *et al.*, *Neuron* **8**, 531 (1992).
3. N. E. Schoppa, K. McCormack, M. A. Tanouye, F. J. Sigworth, *Science* **255**, 1712 (1992).
4. F. J. Sigworth, *Q. Rev. Biophys.* **27**, 1 (1994).
5. N. Yang and R. Horn, *Neuron* **15**, 213 (1995).
6. J. R. Lakowicz, *Principles of Fluorescence Spectroscopy* (Plenum, New York, 1983).
7. S. R. Durell and H. R. Guy, *Biophys. J.* **62**, 238 (1992).
8. Defolliculated, injected *Xenopus* oocytes were incubated for 3 to 4 days at 12°C, treated with 1 mM tetraglycine maleimide (TGM) in MBSH [88 mM NaCl, 1 mM KCl, 0.41 mM $CaCl_2$, 0.33 mM $Ca(NO_3)_2$, 0.82 mM $MgSO_4$, 2.4 mM $NaHCO_3$, and 10 mM Hepes (pH 7.5)] for 1 hour at 21°C to block native membrane sulfhydryls, incubated for 12 to 14 hours at 21°C to permit channels to reach the plasma membrane, and labeled with 5 μM TMRM (Molecular Probes) in K^+-MBSH [100 mM KCl, 1.5 mM $MgCl_2$, 0.5 mM $CaCl_2$, and 10 mM Hepes (pH 7.5)] for 30 min on ice. Two-electrode voltage clamping was with a Dagan CA-1 amplifier in MBSH or in NMGMES [110 mM NMGMES (*N*-methyl-D-glucamine methanesulfonic acid), 1 mM $Ca(MES)_2$, and 10 mM Hepes (pH 7.1)]. Whole-cell gating charge was calculated by subtraction of the linear capacitative component from the integral of the off-gating current. Confocal images were acquired with a Bio-Rad MRC-1000 inverted confocal microscope in photon counting mode with a 20× objective.
9. E. Perozo, R. MacKinnon, F. Bezanilla, E. Stefani, *Neuron* **11**, 353 (1993).
10. T. Hoshi, W. N. Zagotta, R. W. Aldrich, *Science* **250**, 533 (1990).
11. A. Kamb, J. Tseng-Crank, M. A. Tanouye, *Cell* **50**, 405 (1987).
12. Abbreviations for the amino acid residues are as follows: A, Ala; C, Cys; D, Asp; F, Phe; H, His; I, Ile; K, Lys; L, Leu; M, Met; N, Asn; P, Pro; Q, Gln; R, Arg; S, Ser; T, Thr; V, Val; and W, Trp.
13. L. Santacruz-Tolosa, Y. Huang, S. A. John, D. M. Papazian, *Biochemistry* **33**, 5607 (1994).
14. L. M. Mannuzzu, M. M. Moronne, E. Y. Isacoff, data not shown.
15. L366C had a half-maximal voltage of activation of −53.8 ± 1.8 mV (mean ± SEM; n = 5), indicating that channels would be mainly activated during the TMRM incubation.
16. L. C. Timpe, Y. N. Jan, L. Y. Jan, *Neuron* **1**, 659 (1988); E. Y. Isacoff, D. Papazian, L. Timpe, Y. N. Jan, L. Y. Jan, *Cold Spring Harbor Symp. Quant. Biol.* **55**, 9 (1990); L. E. Iverson and B. Rudy, *J. Neurosci.* **10**, 2903 (1990); T. Hoshi, W. N. Zagotta, R. W. Aldrich, *Neuron* **7**, 547 (1991).
17. Fluorescence was measured with a Hamamatsu HC120-05 photomultiplier tube connected to a Nikon DIAPHOT-TMD inverted microscope with TMD-EF Epi-Fluorescence Attachment and a Chroma High Q TRITC filter, and it was digitized at 20 kHz and low-pass filtered at 1 kHz with an 8-pole Bessel filter. Each response is an average of 5 to 10 traces.
18. In solution, replacement of 50 mM KCl of K^+-MBSH with 50 mM KI decreased peak fluorescence of 5 μM TMRM by 40%.
19. E. Stefani, L. Toro, E. Perozo, F. Bezanilla, *Biophys. J.* **66**, 996 (1994); F. Bezanilla, E. Perozo, E. Stefani, *ibid.*, p. 1011; D. Sigg, E. Stefani, F. Bezanilla, *Science* **264**, 578 (1994); W. N. Zagotta, T. Hoshi, R. W. Aldrich, *J. Gen. Physiol.* **103**, 321 (1994).
20. K. McCormack, W. J. Joiner, S. H. Heinemann, *Neuron* **12**, 301 (1994).
21. W. N. Zagotta, T. Hoshi, J. Dittman, R. W. Aldrich, *J. Gen. Physiol.* **103**, 279 (1994).
22. S. K. Aggarwal and R. MacKinnon, *Biophys. J.* **68**, A138 (1995).
23. S. L. Slatin, X.-Q. Qiu, K. S. Jakes, A. Finkelstein, *Nature* **371**, 158 (1994).
24. N. Unwin, *ibid.* **373**, 37 (1995).

25. We thank L. Y. Jan, H. Lecar, J. Ngai, E. Reuveni, O. Baker, R. Harris, H. P. Larsson, and K. Zito for valuable discussion; A. Glazer for advice about fluorescence; G. Westheimer for advice on optical filters; and Technical Instruments Corporation for loan of fluorescence microscopy equipment. ShH4 (W434F/Δ6-46) was provided by L. Toro, and the antibody for the immunoprecipitation was provided by L. Y. Jan. Supported by American Heart Association–California Affiliate grant 94-216, by a McKnight Scholar Award to E.Y.I., and by U.S. Department of Energy contract DE-AC03-76SF00098 to M.M.M.

5 September 1995; accepted 20 November 1995

Activation of Ventrolateral Preoptic Neurons During Sleep

J. E. Sherin, P. J. Shiromani, R. W. McCarley, C. B. Saper*

The rostral hypothalamus and adjacent basal forebrain participate in the generation of sleep, but the neuronal circuitry involved in this process remains poorly characterized. Immunocytochemistry was used to identify the FOS protein, an immediate-early gene product, in a group of ventrolateral preoptic neurons that is specifically activated during sleep. The retrograde tracer cholera toxin B, in combination with FOS immunocytochemistry, was used to show that sleep-activated ventrolateral preoptic neurons innervate the tuberomammillary nucleus, a posterior hypothalamic cell group thought to participate in the modulation of arousal. This monosynaptic pathway in the hypothalamus may play a key role in determining sleep-wake states.

Clinical observations made at the beginning of this century indicated that an intact rostral hypothalamus is critical for the production of normal sleep in humans (*1*). Subsequent experimental studies in animals demonstrated that lesions in the preoptic area and adjacent basal forebrain (POA-BF) cause insomnia (*2*), whereas chemical or electrical stimulation of this region causes sleep (*3*, *4*). Although neurons that are selectively active during sleep have been identified in the POA-BF (*5*, *6*), no such population with an implied role in sleep generation has been anatomically characterized. Because FOS protein accumulates in recently activated neurons (*7*), we immunocytochemically examined the expression of FOS in the brains of 20 rats whose spontaneous sleep-wake behaviors were recorded (*8*), in order to identify sleep-activated cell groups. Animals were killed during the light cycle at 10:00 (n = 8) or 16:00 (n = 7) or during the dark cycle at 22:00 (n = 5), after which their brains were processed for immunocytochemical visualization of FOS protein (*9*).

In agreement with published reports (*10*), we observed fewer FOS-immunoreactive (FOS-ir) neurons in brains from animals that were killed during the light cycle, when rats sleep, than in brains from animals that were killed during the dark cycle, when rats are awake. However, two structures thought to mediate circadian rhythms [the intergeniculate leaflet (IGL) and the dorsal suprachiasmatic nucleus (SCNd)] and a group of cells in the ventrolateral preoptic area (VLPO) showed a pronounced and focal increase in the number of FOS-ir cells in brains from animals killed during the light cycle as compared with the dark cycle (*11*). Although the IGL and SCNd consistently contained numerous FOS-ir cells in the brains of all animals killed during the light cycle, the number of FOS-ir cells in the VLPO of these animals was less consistent and seemed more closely related to

J. E. Sherin, Department of Neurology, Harvard Medical School, Beth Israel Hospital, Boston, MA 02215; Program in Neuroscience, Harvard Medical School, Boston, MA 02115; and Committee on Neurobiology, University of Chicago, Chicago, IL 60637, USA.
P. J. Shiromani and R. W. McCarley, Program in Neuroscience, Harvard Medical School, Boston, MA 02115, and Department of Psychiatry, Harvard Medical School, Brockton Veterans Administration Hospital, Brockton, MA 02401, USA.
C. B. Saper, Department of Neurology, Harvard Medical School, Beth Israel Hospital, Boston, MA 02215, and Program in Neuroscience, Harvard Medical School, Boston, MA 02115, USA.

*To whom correspondence should be addressed at the Department of Neurology, Beth Israel Hospital, 330 Brookline Avenue, Boston, MA 02215, USA. E-mail: csaper@bih.harvard.edu